Auton Robot (2010) 29: 119–135
DOI 10.1007/s10514-010-9186-z

Passive joint stiffness in the hip and knee increases the energy efficiency of leg swinging

Shane A. Migliore · Lena H. Ting · Stephen P. DeWeerth

Received: 1 April 2009 / Accepted: 29 March 2010 / Published online: 23 April 2010

Abstract In the field of minimally-actuated robots, energy efficiency and stability are two of the fundamental criteria that can increase autonomy and improve task-performance capabilities. In this paper, we demonstrate that the energetic cost of leg swinging in dynamic robots can be reduced without significantly affecting stability by emulating the physiological use of passive joint stiffness, and we suggest that similar efficiency improvements could be realized in dynamic walking robots. Our experimental model consists of a two-segment dynamically swinging robotic leg with hip and knee joints. Closed-loop control is provided to the hip using neurally inspired, nonlinear oscillators that do not override the leg's natural dynamics. We examined both linear and nonlinear, physiologically based stiffness profiles at the hip and knee and a hyperextension-preventing hard stop at the knee. Our results indicate that passive joint stiffness applied at one or both joints can improve the energy efficiency of leg swinging by reducing the actuator work required to counter gravitational torque and by promoting kinetic energy transfer between the shank and thigh. Energetic cost reductions (relative to the no-stiffness case) of approximately 25% can be achieved using hip stiffness, provided that the hip actuation bias angle is not coincident with gravity, and cost reductions of approximately 66% can be achieved using knee stiffness. We also found that constant stiffness combined with a limit on knee hyperextension produces comparable results to the physiological stiffness model without requiring complex implementation techniques. Although this study focused on the task of leg swinging, our results suggest that passive-stiffness properties could also increase the energy efficiency of walking by reducing the cost of forward leg swing by up to 66%. We also expect that the energetic cost of walking could be further reduced by adding stiffness to the ankle to assist in the propulsive portion of stance phase.

Keywords Passive dynamics · Joint stiffness · Antagonistic actuation · Walking robots

1 Introduction

Energy conservation is an important consideration in animal locomotion, as it often dictates or at least influences the form of movements that are used to perform a behavior (Sparrow et al. 2000). For example, the transition between gaits as animals change speed often occurs when the energy required to remain in the current gait increases beyond that of an available alternate gait (Sasaki and Neptune 2006). The two primary energy-conserving mechanisms in human walking are (1) the passive transfer of kinetic and gravitational potential energy (Cavagna and Margaria 1966) and (2) the passive storage and release of energy by elastic tissue components (McMahon et al. 1987; Blickhan 1989; Hof 1990). Using the inverted pendulum model of walking, it has been shown that the maximum theoretical efficiency of the first energy saving mechanism is only 65%, leaving a substantial amount of energy to be either lost or stored and reused by passive elastic components (Sasaki and Neptune 2006). The vast majority of walking robots lose this energy by ignoring the potential benefit of using passive elastic components at their joints. In this paper, we first describe

S.A. Migliore
School of Electrical and Computer Engineering, Georgia Institute of Technology, Atlanta, GA, USA

L.H. Ting · S.P. DeWeerth (✉)
Department of Biomedical Engineering, Emory University/Georgia Institute of Technology, Atlanta, GA, USA
e-mail: steve.deweerth@gatech.edu

the role of passive stiffness in current robot actuation systems. We then detail how animals use the passive-stiffness properties of muscle to improve their locomotion efficiency. Finally, we present a series of experiments that analyze the benefit elastic energy storage can provide passive-dynamic robots during leg swinging. We demonstrate that passive stiffness applied at the hip or knee or both can lower the energetic cost of leg swinging (1) by promoting the efficient transfer of mechanical energy and (2) by assisting the actuators in producing anti-gravity joint torques.

2 Background

Bipedal robots are typically designed using either the trajectory-control approach, which rigidly dictates joint angles, or the passive-dynamic approach, which uses no actuators and requires a small downhill slope for input energy.

Trajectory-control robots have traditionally been focused primarily on task/behavior performance (e.g., walking, running, balancing, hopping). As a result, the designers have chosen to place a low priority on energy efficiency, opting instead to use inefficient, highly geared actuators to achieve precision movements (Hirai et al. 1998; Yamaguchi and Takanishi 1997; Ogura et al. 2004; Loffler et al. 2002; Endo et al. 2005; Kaneko et al. 2004; Kim et al. 2005). In general, relatively high work rates are required in these robots because the frequencies of their movements are not matched to the corresponding limbs' natural frequencies. For robots that perform stereotypical, rhythmic movements such as walking, passive elasticity could be used to alter a joint's natural frequency such that the difference between the desired movement frequency and the natural frequency is reduced. This reduction would lower the actuation work required (Doke et al. 2005) and improve the robot's efficiency for this task. Passive elasticity could also be used to reduce actuator loads by assisting with anti-gravity movements.

Passive-dynamic robots (McGeer 1990a, 1990b) have the potential to use passive joint stiffness to alter their natural dynamics, energy efficiency, and stability, but this approach has not yet been thoroughly explored and has not yet been tested in physical implementations of this type of robot. Previous passive-dynamic walking robots have operated with an energy efficiency approximately equal to that of human walking (Collins and Ruina 2005). By adding minimal actuation, these robots can increase their stability region by expanding the range of initial and environmental conditions that can be tolerated while still maintaining an appropriate level of mechanical energy. The key to efficiency in these robots, though, is to use actuator work sparingly so that movements can follow the natural leg dynamics and remain largely passive throughout much of the gait cycle. Series-elastic actuation (Williamson 1995; Pratt and Williamson 1995) is one method used to minimize actuator work and has been used previously in non-passive-dynamic robotic devices (Wisse et al. 2007; Migliore et al. 2005, 2007; Yamaguchi and Takanishi 1997; Kolacinski and Quinn 1998; Robinson et al. 1999). By emulating the series (active) elastic component from the Hill muscle model (Hill 1970), this technique reduces the parasitic effect of actuators, freeing the leg to move naturally. The parallel (passive) elastic component from the Hill muscle model provides joints with elasticity that is independent of actuator output. In animals, the parallel elastic component models the intramuscular connective tissue and generally provides the majority of the passive force production (Brinckmann et al. 2002). This study explores whether dynamic robots can exploit this parallel elastic component to improve the energy efficiency of physical movements.

The inspiration for incorporating passive elasticity in walking robots comes from animals, which use their muscles and tendons as both actuators and sources of compliance (i.e., the inverse of stiffness) for joints. Actuation is used to produce voluntary movements and to modify natural movements, such as those that occur during passive-dynamic leg swinging. Musculotendon compliance allows joint movements to be influenced by natural limb dynamics and by the environment. Musculotendon compliance also provides animals with the ability to temporarily store energy during one phase of a movement so that it can be recovered at a later phase when it is useful for the behavior being performed. For example, in human walking, elastic energy is stored in the Achilles tendon and the arch of the foot during stance. At toe-off, this passively stored energy is used to supplement active muscle torque such that only a portion of the total push-off force produced by the ankle requires the expenditure of active energy. The amount of mechanical energy stored and released passively during human walking has been estimated to be as much as 50% of the body's total mechanical energy (Alexander and Bennet-Clark 1977; Ker et al. 1987).

Animals store and release energy from passive elastic components to reduce the metabolic costs associated with rhythmic movement. Without passive energy storage, quickly reversing a leg's swing direction would require muscles to actively produce negative work to decelerate the leg and then to produce positive work to accelerate it in the opposite direction. Both phases cost energy: negative work expends energy as heat dissipation, and positive work requires the consumption of metabolic energy. Passive elasticity reduces the energy demand by storing energy during the negative work phase and releasing energy during the positive work phase. Although this mechanism is not 100% efficient and still requires supplemental active muscle work, the total level of metabolic energy required to perform the behavior is reduced.

In addition to providing a means of efficiently storing and releasing energy, passive stiffness is also used by animals to prevent injuries and to stabilize motion (Wheeless 2005). Passive joint stiffness results from the physical properties of the muscles that span it. The lengths, attachment points, and passive tensile forces of all such muscles vector sum to produce a passive-stiffness trajectory that is a function of the joint angle and, in the case of multiarticular muscles, of the neighboring joint angles. Because the resting length of muscles generally lie within the middle of the actuated joint's range of motion, passive restoring torques are generally directed away from extreme angles.

The goal of this research was to study the efficacy of passive (actuator-independent) elasticity in reducing the actuator work required to produce leg swinging. Specifically, we tested the following hypotheses:

- The addition of passive hip stiffness to a compliant swinging leg can reduce energetic cost by producing anti-gravity torques that lower the amount of actuator work required for leg swinging.
- The addition of passive knee stiffness to a compliant swinging leg can reduce energetic cost by promoting the efficient transfer of kinetic energy between the shank and thigh during swinging movements, increasing the stride length.

3 Swinging leg model

To study the dynamics of human leg swinging, a model of a full-scale adult female human leg was developed and was implemented both computationally and robotically. The computational implementation allowed us to quickly analyze the effect of individual control system parameters on system behavior; the robotic implementation allowed us to validate the computational results in a physically realistic setting that is directly applicable to legged robots. The model was designed anthropomorphically such that the limb segments' mass, length, center of mass, and moment of inertia closely matched the target human leg. A full description of the leg model can be found in Migliore (2008). The robotic implementation of the leg model is shown in Fig. 1.

The leg model has a biologically inspired control system that uses a neural central pattern generator (CPG) (Brown 1914) based on the Matsuoka Half-Center Oscillators (HCO) (Matsuoka 1985, 1987). The hip joint is actuated with one HCO and the knee is left passive. We chose not to actively control the knee in these experiments so that comparisons could be made with existing walking robots that use passive knees (Wisse et al. 2007; Collins and Ruina 2005) and so that predictions regarding the potential benefit of using passive stiffness with these robots. All inter-joint synchronization that occurs as the leg swings is a result of the mechanical coupling between the joints and angular feedback from the hip joint to the HCO. The sensory feedback between the hip and the HCO allows the HCO's oscillation frequency to entrain to the mechanical resonant frequency of the mechanical system. This behavior, called *resonance tuning*, is seen in biological systems (Hatsopoulos 1996; Abe and Yamada 2003; Rossignol 1996) and is common in rhythmically controlled movement and has been studied previously in robotic systems (Simoni 2002; Williams and DeWeerth 2007). As in many legged animals (including humans), our model also includes an asymmetric limit to knee-angle extension that prevents the knee from extending more than a few degrees past the anatomical position (i.e., straight leg). In humans, this restriction is caused by knee flexion muscles and the physical construction of the knee, including stabilizing ligaments such as the anterior cruciate ligament.

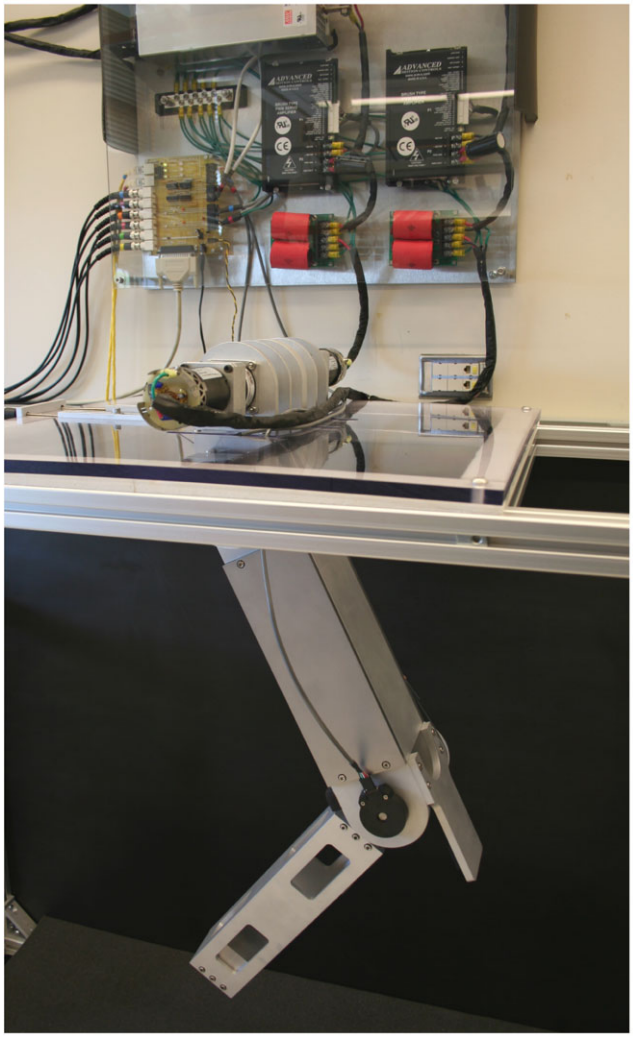

Fig. 1 Robotic implementation of the swinging leg model

Parameter values were chosen in various ways. Most of the HCO parameters were selected using published val-

Table 1 Ideal mechanical properties of each leg segment. The center of mass and moment of inertia are referenced from the proximal extent of the segment

Segment	Length (cm)	Mass (kg)	CoM (cm)	MoI (kg m^2)
Thigh	40.4	6.24	17.5	0.297
Shank/foot	47.0	3.81	28.5	0.454
Total leg	87.4	10.1	39.0	2.40

ues know to work well for the control of robotic systems (Williamson 1999). The leg mass properties were chosen by determining the anthropologically appropriate values (Table 1). The values for the initial conditions were chosen so that the leg was initiated with an acceptable energy level. The remaining parameters were chosen using 2,500-trial Monte Carlo optimizations that minimized the energetic cost required to track the HCO outputs.

Physical implementation was used because this research is intended to be directly applicable to the improvement of legged robotics. In addition, the physical implementation necessarily includes real-world imperfections such as parameter mismatch, difficult-to-model friction, and signal noise. In this implementation, the robotic leg swings freely with its hip mechanically grounded to a supporting platform. DC motors directly drive each joint via cables. The gear ratio of the motors was kept low to minimize the parasitic effects of motor friction, damping, and inertia at the joints. *Virtual model control* (Pratt et al. 1997) was used to implement passive viscoelasticity at the joints by computationally modeling the effects of passive components. These virtual components use real-time feedback information from the leg and apply their resultant torque to the joints using the actuating motors.

The two primary criteria that are used to judge the performance of the swinging leg are energy efficiency and stability. Energy efficiency is evaluated using the *specific cost of leg swinging*—a quantity derived from the definition of the *specific cost of transport* (Kram and Taylor 1990)—and is defined as the energy required to swing a unit mass leg a unit stride length:

$$\sigma = \frac{E_\mathrm{m}}{MgL_\mathrm{s}} \tag{1}$$

where σ is the specific cost of leg swinging, E_m is the active energy injected into the leg by the motor, M is the mass of the swinging leg, and L_s is the leg's stride length (i.e., the horizontal distance that the leg's center of mass travels during a single stride). For brevity, we refer to the specific cost of leg swinging as *energetic cost* for the remainder of this paper. The stability of the leg is determined using Poincaré sections and Floquet theory (Strogatz 1994; Nayfey and Balachandran 1995). The maximum Floquet multiplier, MFM, is calculated empirically using a sequence of perturbations to the system, and the system is deemed stable if $|MFM|$ is less than unity.

4 Methods

Experiments were performed on two systems—a single pendulum and the complete leg model (i.e., a double pendulum with knee-angle asymmetry). The single pendulum was tested because it provided a simple means of exploring the fundamental behavior and performance limitations of this type of neurally controlled, closed-loop system. For each configuration, we examined the energetic cost reduction that occurred with the use of either a simple, constant joint stiffness or a more complex, variable stiffness profile, which emulates the true passive-stiffness properties of the human leg.

For each experiment, the following three variables were investigated:

- θ_ab [rad] is the actuation bias angle, or the joint angle about which the HCO feedback is biased
- θ_sb [rad] is the stiffness bias angle, or the joint angle about which the passive-stiffness function is biased
- K [Nm/rad] is the gain of the passive-stiffness function

For clarity, θ_ab and θ_sb are assumed to be non-negative (i.e., correspond to flexion angles) for all analysis in this paper (Fig. 2).

4.1 Passive elasticity

Constant joint stiffness was implemented by applying linear elastic elements (e.g., normal linear springs) that produced the following joint torques:

$$\Gamma_\mathrm{s,h} = K_\mathrm{h}(\theta_\mathrm{h} - \theta_\mathrm{sb,h}) \tag{2}$$

$$\Gamma_\mathrm{s,k} = K_\mathrm{k}(\theta_\mathrm{k} - \theta_\mathrm{sb,k}) \tag{3}$$

where $\Gamma_\mathrm{s,h}$ and $\Gamma_\mathrm{s,k}$ are the stiffness torques applied at the hip and knee, and K_h and K_k are the gains of the hip and knee stiffness functions.

Variable joint stiffness was implemented as a nonlinear trajectory that, as in humans, varies smoothly as a function of joint angle. We chose to use an existing model that was developed by curve-fitting empirically measured human data (Riener and Edrich 1999). This "Physiological Model" incorporates uniarticular and biarticular muscles such that the passive stiffness of each joint is a function of both hip and knee angle. Although we planned to incorporate the effects of biarticular muscles, this model's stiffness functions were path dependent and not energy conserving, making

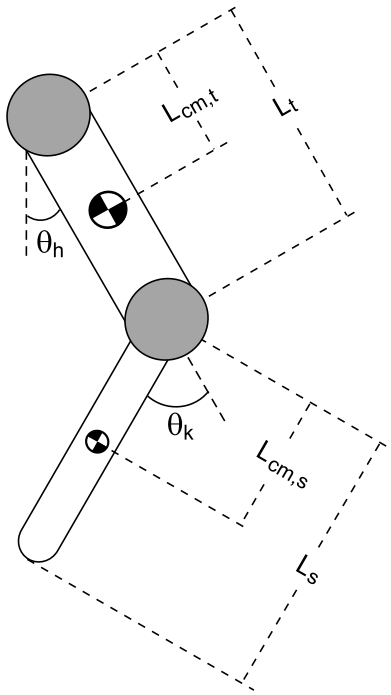

Fig. 2 Mass properties and angle definitions of the swinging leg model. L_t and L_s represent the length of the thigh and shank, respectively. $L_{cm,t}$ represents the distance from the hip to the thigh center of mass. $L_{cm,s}$ represents the distance from the knee to the shank center of mass. θ_h represents the angle of the thigh relative to the vertical. θ_k represents the angle of the shank relative to the thigh

analysis of elastic energy storage difficult. We chose to simplify the Physiological Model by removing the stiffness contribution made by biarticular muscles. To remove the contribution, we chose angles for each joint that were at the midpoint of their typical range of motion and used these values for the "biarticular" joint angle each time stiffness was calculated. The modified equations of the Physiological Model that we used to implement variable joint stiffness are:

$$\Gamma_{s,h} = K_h\left(4.05e^{-4.30\theta_h} - 2.43e^{1.75\theta_h} + 8.07\right) \tag{4}$$

$$\Gamma_{s,k} = K_k\left(7.52e^{-2.02\theta_k} - 0.02e^{2.84\theta_k} + 9.21e^{-8.60\theta_k} - 4.82\right) \tag{5}$$

where the coefficients in the arguments of the exponents are unitless and all remaining coefficients and constants are in units of radians. The effective bias angle of each curve, $\theta_{sb,h}$ and $\theta_{sb,k}$, were found by determining the joint angle at which stiffness torque is zero.

To avoid complex implementation issues in the robotic model, we used *virtual model control* to actively implement both forms of passive stiffness. We ignored the energy needed to implement passive stiffness when calculating the energetic cost because these passive-stiffness components do not require external energy when attached physically. Therefore, we chose not to penalize the energetic cost of our experimental leg controller based on our experimental implementation method.[1]

Table 2 Canonical parameters used for the single pendulum experiments

Description	Parameter	Canonical value
HCO time constant	τ_1	0.75 sec
Joint damping	B	0.14 Nm sec/rad
Feed-forward gain	G_{ff}	9.50
Feedback gain	G_{fb}	10.50

4.2 Single pendulum model

We assessed the potential benefit of incorporating passive-stiffness properties into robotic joints by first reducing the leg model to a single-degree-of-freedom pendulum. This was done by locking the knee such that the pendulum had the mass properties of the entire leg ($M = 10.80$ kg, $L = 0.864$ m, $L_{cm} = 0.371$ m, $J = 0.846$ kg m^2). We chose values for the remaining system parameters by removing passive stiffness from the model and performing a optimization (Table 2). Stiffness was removed for the optimization so that the canonical parameter set would be independent of the stiffness function chosen.

4.3 Double pendulum model

The only difference between the single- and double-pendulum models is the ability for the knee to bend during leg swing. For consistency with the single-pendulum model, the double pendulum used all of the same parameter values listed in Table 2. With the knee able to bend, the value of an additional parameter—knee damping (B_k)—had to be determined. We found that setting B_k equal to 1.00 Nm/rad provided a balance of low energetic cost, reasonable maximum Floquet multiplier value (0.71), and underdamped motion that produces significant knee rotation (± 0.32 rad). Lower damping values produced lower energetic costs but moved the system closer to instability. Higher damping values caused the knee to become overdamped and limited its movement.

Double pendulum experiments were performed both with and without asymmetric restrictions on knee angle. In humans, two mechanisms are responsible for knee-angle asym-

[1] Despite our method of calculating energetic cost for this research, true energetic cost reduction can only occur when passive stiffness is indeed implemented passively. At present, few techniques exist that can passively produce arbitrary joint stiffness profiles (Migliore et al. 2007; English and Russell 1999).

metry: (1) a gradual restriction provided by passive muscle properties and (2) a hard stop provided by the physical construction of the knee (e.g., the anterior cruciate ligament) (Piazza and Delp 1995). In the initial experiments, we did not include the hard-stop component; we relied completely on passive stiffness to prevent hyperextension. We then added the hard stop and compared the performance.

To model the knee-angle hard stop, we chose a high-stiffness element that begins applying torque when the knee is near full extension and rapidly increases torque output as extension increases. We modeled the hard stop according to the following equation:

$$\Gamma_{\mathrm{HS}} = 1.0\ \mathrm{Nm/rad} \cdot e^{-15.0\,\theta_{\mathrm{k}}} \tag{6}$$

where Γ_{HS} is the torque produced by the knee-angle hard stop.

4.4 Experimental technique

We first collected baseline data for the single pendulum by removing passive stiffness from the joint and by measuring the effect θ_{ab} had on both the energetic cost and the stability (maximum Floquet multiplier) of the system. We then added constant passive stiffness to the joint and determined if regions in the θ_{ab}, θ_{sb}, K parameter space existed such that the energetic cost was reduced without significantly reducing stability (increasing the maximum Floquet multiplier).

From (1), energetic cost is minimized when the pendulum produces large strides with minimal active energy. Therefore, the energetic cost increases (1) when the oscillation amplitude diminishes, which produces smaller a stride length or (2) when the center of the oscillation becomes offset from θ_{ab}, which increases the feedback (error) signal to the controller and causes the controller to produce higher levels of active energy (actuator work).

To determine whether the single pendulum system could benefit from the use of variable passive stiffness, we replaced the constant stiffness function with the physiologically based model. We used the variable hip stiffness function for the single pendulum because the mass properties of this pendulum were chosen to match those of the entire leg. Parameter searches with the variable stiffness were limited to the K, θ_{ab} parameter space because θ_{sb} is fixed by the stiffness model.

A similar experimental procedure was followed with the double pendulum. Baseline data was collected by removing stiffness from the hip and knee and sweeping θ_{ab}. Then, the following experimental conditions were assessed both with and without the hard knee stop included: (1) constant stiffness at the hip only, (2) constant stiffness at the knee only, (3) constant stiffness at both joints, (4) variable stiffness at the hip only, (5) variable stiffness at the knee only, and (6) variable stiffness at both joints.

Several experimental permutations exist for both the single and double pendulums, such as which stiffness function to use and which parameters to sweep. To simplify testing, we assessed the performance of each system using a two-step process. The first step was to fix the value of θ_{ab} to either a zero or non-zero value and then to sweep the values of each stiffness parameter. (For the non-zero value, we chose $\theta_{\mathrm{ab}} = 0.15$ rad because this value approximates the center of the hip's range of motion during normal human walking (Hurmuzlu et al. 1994).) This step was used to quickly identify good operating regions and behavioral trends. The second step was to fix the stiffness parameters and sweep θ_{ab}. This step provided a more detailed understanding of how energetic cost, stability, and HCO output were affected by the choice of actuation bias angle.

5 Results

The energetic cost of swinging either the single or double pendulum can be reduced by applying stiffness at one or both joints. Energetic cost reductions (relative to the no-stiffness case) of approximately 25% can be achieved using hip stiffness, provided that θ_{ab} is non-zero, and cost reductions of approximately 66% can be achieved using knee stiffness (with the double pendulum).

5.1 Single pendulum model

Both constant and variable passive-stiffness functions are capable of reducing the energetic cost; the amount of reduction is a function of θ_{ab} and the stiffness-function parameter(s). The variable stiffness provides no benefit that warrants its complicated implementation, and neither stiffness function significantly affects the stability of the system. These results are presented in detail in the remainder of this section.

Figure 3A presents the effect that constant passive stiffness has on the system when θ_{ab} is zero. Regardless of the stiffness parameter values, the inclusion of constant passive stiffness results in an increased energetic cost. This cost increase occurs for two distinct reasons: (1) when θ_{sb} is zero, the passive stiffness pulls the pendulum towards the origin ($\theta = 0$ rad), restricting oscillation amplitude and (2) when θ_{sb} is non-zero, the passive stiffness pulls the pendulum asymmetrically away from θ_{ab}, increasing feedback signal magnitude (and therefore increasing actuator work). In either case, energetic cost increases in a manner directly related to K.

When θ_{ab} is non-zero, the pendulum joint requires additional torque to oscillate symmetrically about θ_{ab} because gravity pulls asymmetrically towards the origin. In the absence of passive stiffness, gravity causes the pendulum to

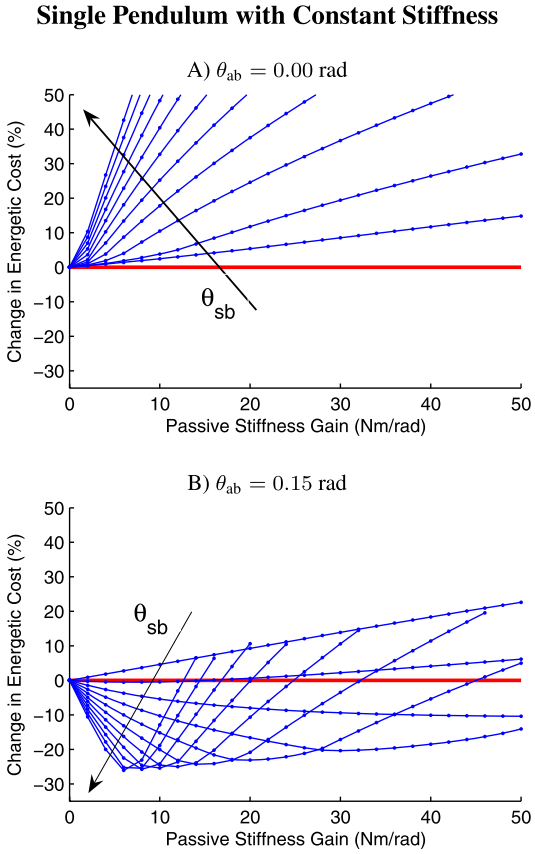

Fig. 3 Effect of actuation bias angle on energetic cost reduction in the single pendulum. (**A**) With $\theta_{ab} = 0.00$ rad, any constant stiffness function, regardless of parameters chosen, increases energetic cost. (**B**) With $\theta_{ab} = 0.15$ rad, constant stiffness is capable of reducing energetic cost, given appropriate parameter regions. The individual traces in each plot correspond to fixed values of θ_{sb}. The *arrows* indicate the effect of increasing θ_{sb} from 0.00 to 1.00 rad in increments of 0.10 rad

oscillate about an angle between zero and θ_{ab}. In this case, actuator torque is used asymmetrically to "flex" the pendulum's joint toward θ_{ab} and gravity provides all of (or most of) the restoring torque. When gravity provides all of the restoring torque, the CPG controller's output becomes uniphasic such that a non-zero output occurs only during the flexion phase of the oscillation.[2]

Figure 3B presents the effect that constant passive stiffness has on the system with $\theta_{ab} = 0.15$ rad. Adding passive stiffness in this case can either reduce or increase the energetic cost depending on the relationship between θ_{ab} and θ_{sb} and on the value of K. When θ_{sb} is small relative to θ_{ab}, the stiffness assists gravity in pulling the pendulum away from θ_{ab}, causing the energetic cost to increase (e.g., the top trace in Fig. 3B). As θ_{sb} increases, the stiffness begins to counter the gravitational effect by storing elastic potential energy as the pendulum joint extends toward the origin and releasing it as the pendulum joint flexes. By countering gravity, this passive elasticity reduces the level of active energy used and therefore lowers the energetic cost (e.g., the bottom traces in Fig. 3B).

Figure 3 was most useful in determining ranges of parameters that produced energetic cost reduction. Figure 3A demonstrates that passive stiffness is not beneficial regardless of parameter values when θ_{ab} is aligned with gravity. Figure 3B demonstrates that when $\theta_{ab} = 0.15$ rad, energetic cost is minimized when the passive-stiffness function uses high values for θ_{sb} and low values for K. The maximum level of energetic cost reduction saturates at about 26% with $\theta_{sb} = 1.0$ rad and $K = 6.0$ Nm/rad. Increasing θ_{sb} above 1.0 rad can further reduce energetic cost by 1.5%, but doing this significantly reduces the range of K values that produce energetic cost reduction.

Figure 4 shows the effects θ_{sb} and K have on the performance of the single pendulum as θ_{ab} is varied. The values of θ_{sb} and K used for these experiments were chosen using the beneficial parameter ranges from Fig. 3B as a guideline. The energetic cost reduction plots (Figs. 4A and 4B) show that as either K or θ_{sb} increase, the potential reduction in energetic cost increases, along with the value of θ_{ab} at which the reduction is maximized. The stability plots (Figs. 4C and 4D) show that increasing K moves the system towards instability, while increasing θ_{sb} maintains the overall stability level. (Stability is discussed in more detail later in this section.)

Figure 4 demonstrates that three distinct operating regions exist in this system. The first region, which has already been discussed, occurs when $\theta_{sb} \ll \theta_{ab}$ and all actuator torque is used to flex the joint away from the origin towards θ_{ab}. This region is characterized by a uniphasic CPG output and can be seen as the flat regions to the left of the troughs in Figs. 4C and 4D. Within this region, increasing θ_{sb} reduces the level of energetic cost because the stiffness begins countering the gravitational torque, which reduces actuator work. The second region occurs as θ_{sb} continues to increase and passive-stiffness torques approximately counter the gravitational torque. This operating region is characterized by a biphasic CPG controller output and can be seen as the troughs in Figs. 4C and 4D. At some value of θ_{sb}, the two phases of the CPG controller output are symmetric. This operating point occurs at the trough minima in Figs. 4A and 4B and represents the value of θ_{sb} that produces the most energetically efficient and stable oscillation dynamics (given values for θ_{ab} and K). When θ_{sb} is slightly above or below this value, the CPG controller maintains biphasic output but the duty cycle of the phases are unequal, the energetic cost is higher, and the stability is reduced. The third operating region occurs when $\theta_{sb} \gg \theta_{ab}$ and all actuator torque

[2]Uniphasic behavior is possible because the output of a Matsuoka oscillator is the difference of two half-wave rectified "neuron" output signals, and strongly asymmetric feedback can drive one of these signals low enough that it never exceeds zero.

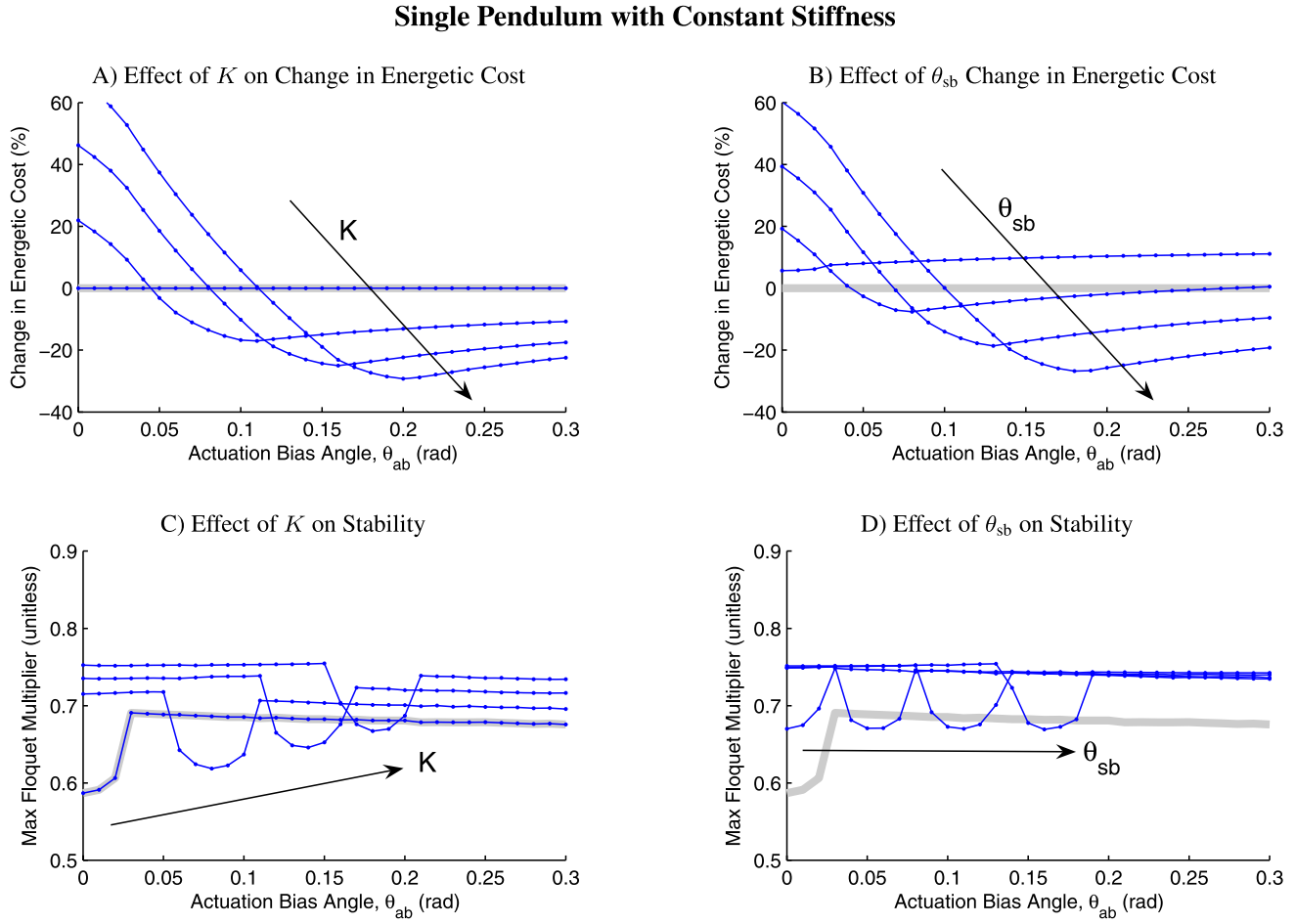

Fig. 4 Effect of constant passive stiffness on the energetic cost reduction (plots (**A**) and (**B**)), and stability (plots (**C**) and (**D**)) of single pendulum swinging. Plots (**A**) and (**C**) demonstrate the effect of setting θ_{sb} equal to 0.45 rad and performing tests with K equal to 0.0, 7.0, 14.0, and 21.0 Nm/rad. Plots (**B**) and (**D**) demonstrate the effect of setting K equal to 21.0 Nm/rad and performing tests with θ_{sb} equal to 0.0, 0.15, 0.30, and 0.45 rad. The *arrow* in each plot indicates the direction of increasing the test parameter. The *thick gray lines* indicate the system performance without stiffness applied

is used to extend the pendulum's joint away from θ_{sb} and towards the origin. This region is characterized by a uniphasic CPG output with the sign of the output opposite that of the first region.

The preceding analysis details the effect of sweeping θ_{sb}. Similar performance and operating regions occur when K is swept, provided that θ_{sb} is nonzero. We have chosen not to include the description here for brevity.

The parameters θ_{sb} and K have slightly varying effects on stability. Figures 4C and 4D show that increasing either parameter causes the traces to shift toward larger θ_{ab} values. Increasing K also shifts the traces vertically toward larger maximum Floquet multiplier values, indicating that a side effect of varying stiffness gain is that system stability is reduced. However, the largest increase from baseline was only 14% and this increase did not produce behavioral changes significant enough to be noticed by visual inspection.

Based on the performance of the constant stiffness function, we expected that the variable stiffness function would also be capable of reducing energetic cost because the effective bias angle of the variable stiffness function (0.70 rad) exceeds all tested values of θ_{ab}. The experimental results (Fig. 5) show that variable stiffness affects the energetic cost (Fig. 5A) and stability (Fig. 5B) of pendulum dynamics in a manner qualitatively similar to constant stiffness. Furthermore, all operating regions described for the constant stiffness case (including the energy efficient biphasic region) were replicated with the variable stiffness by varying K_h.

The dashed traces in Fig. 5 demonstrate that the variable stiffness effects can be nearly replicated by constant stiffness with θ_{sb} set equal to the inherent bias angle of the variable stiffness (0.70 rad). Additionally, the maximum energetic cost reduction is approximately the same for the

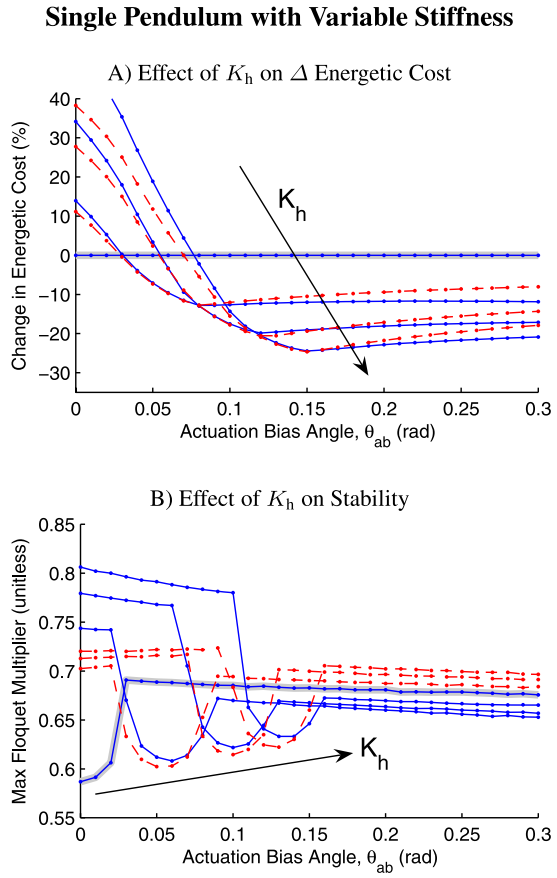

Fig. 5 Effect of variable (physiological) passive stiffness on the energetic cost (**A**) and stability (**B**) of pendulum swinging. The *solid traces* represent the variable stiffness function with K_h set equal to 0.0, 0.15, 0.30, and 0.45 Nm. The *dashed traces* represent the constant stiffness function with $\theta_{sb} = 0.70$ rad and $K_h = 3.00$, 6.00, and 8.00 Nm/rad. Increasing values of K and K_h are indicated by the *arrows* in each plot. The *thick gray lines* indicate the system performance without stiffness applied

variable (25%) and constant (27%) passive-stiffness functions.

5.2 Double pendulum

In Sect. 5.1, we showed that energetic cost can be reduced in the single pendulum only when the actuation bias angle, θ_{ab}, is non-zero. In this section, we demonstrate that in the double pendulum, this property is true only for hip stiffness. Knee stiffness, especially that which prevents knee hyperextension, can provide energetic cost reduction regardless of actuation bias angle.

We did not include analysis of the effects stiffness has on the maximum Floquet multiplier in this section because, as with the single pendulum, the effects were limited and did not significantly influence the dynamics of the system.

As with the single pendulum model, the first experiment was performed to identify regions in parameter space that produce the largest energetic cost reductions for both zero and non-zero values of θ_{ab}. Figures 6A and 6B show that constant stiffness at the hip affects the double pendulum in a manner qualitatively similar to that of the single pendulum. This was expected because the only difference between the two cases is whether the knee is allowed to symmetrically bend.

Knee stiffness has a significantly different effect on the dynamics than hip stiffness (Figs. 6C and 6D). When θ_{ab} is zero, the most energetically beneficial approach is to apply knee stiffness with a zero bias angle and a high gain. This stiffness restricts the magnitude of knee oscillations without expending energy (in contrast to the effects of a damping element) such that the knee remains near the origin. As a result, the double pendulum is able to transfer kinetic and potential energy during swinging with an efficiency closer to that of the single pendulum. Energy is expended in the case of the free-swinging knee because energy is used to hyperextend and hyperflex the knee, and these movements act to diminish stride length and increase the amount of actuator work required to maintain constant-amplitude oscillations. When the knee stiffness bias angle ($\theta_{sb,k}$) is increased, the knee becomes asymmetrically biased towards flexion, and the energetic cost increases. Knee flexion bias causes a cost increase because interaction torques produce a hip flexion bias, and, as a result, the CPG controller expends additional active energy to keep hip-angle oscillations centered about the origin.

When θ_{ab} is non-zero (Fig. 6D), the double pendulum is much more sensitive to changes in the value of the knee stiffness gain (K_k) than to changes in $\theta_{sb,k}$. For the range of parameters tested, increasing K_k reduced the energetic cost by up to 48%; increasing $\theta_{sb,k}$ only reduced the energetic cost by up to 7%. The difference in the magnitude of these effects is a result of the two parameters working in different ways. As K_k is increased, the magnitude of the knee oscillations are restricted, which improves the transfer of mechanical energy. As $\theta_{sb,k}$ is increased, an effective hip bias angle is created (via interaction torques) that promotes hip flexion and reduces the level of active energy expended. The larger effect of changing K_k indicates that efficient mechanical energy transfer is more important than assistive joint torques in reducing energetic cost in this system.

We used Figs. 6B and 6D and similar plots for the variable stiffness (not shown) to determine a canonical set of stiffness parameter values (Table 3) that could be used to compare the relative efficacy of each stiffness implementation. With the exception of the variable hip stiffness gain, we chose the value of each parameter as that which produced the lowest energetic cost. The value of the variable hip stiffness gain was chosen separately because all non-zero values of this parameter produce increased energetic cost, and therefore cost is minimized when the gain is zero.

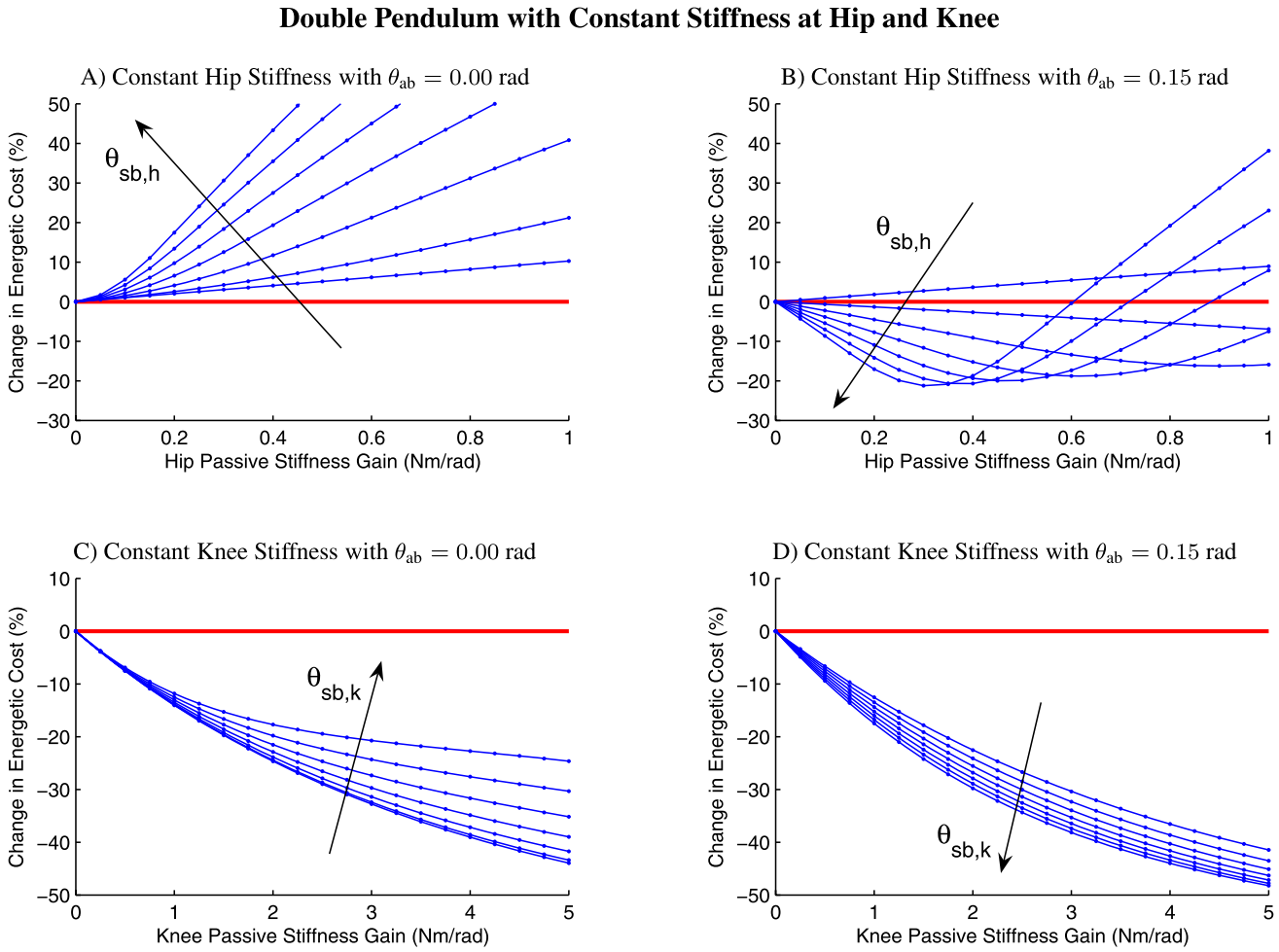

Fig. 6 Change in energetic cost of double pendulum swinging with constant passive stiffness applied to the hip and knee. The individual traces in each plot correspond to fixed values of θ_{sb}. In Plots (**A**) and (**B**), constant stiffness is applied only at the hip, and the knee swings freely with no restrictions applied. The *arrows* indicate the effect of increasing $\theta_{sb,h}$ from 0.00 to 12.00 rad in increments of 2.00 rad. In Plots (**C**) and (**D**), constant stiffness is applied only at the knee. The *arrows* indicate the effect of increasing $\theta_{sb,k}$ from 0.00 to 0.60 rad in increments of 0.10 rad

Table 3 Canonical stiffness parameters used for the double pendulum experiments

Stiffness type	Parameter	Canonical value
Constant	K_h	0.30 Nm/rad
	K_k	4.00 Nm/rad
	$\theta_{sb,h}$	12.00 rad
	$\theta_{sb,k}$	0.60 rad
Variable	K_h	0.30 Nm/rad
	K_k	1.00 Nm/rad

To compare the effect of this parameter with all others, we arbitrarily chose the value of the variable hip stiffness gain to be = 0.30 Nm/rad.

Using the canonical stiffness parameters, we conducted a series of experiments that demonstrate how the various stiffness implementations affect the energetic cost of double pendulum swinging. The results (Fig. 7) indicate that constant hip stiffness, constant knee stiffness, and variable knee stiffness reduce energetic cost and that the amount of reduction can be increased with the application of the knee-angle hard stop. In contrast, the use of variable hip stiffness increases energetic cost.

Constant hip stiffness (Fig. 7A) affects energetic cost in a manner similar to that of the single pendulum: at low values of θ_{ab}, energetic cost is increased because the stiffness asymmetrically pulls the joint away from θ_{ab}, increasing actuator work; at higher values of θ_{ab}, energetic cost decreases in a manner directly related to K_h. The level of energetic cost reduction at higher values of θ_{ab} is increased when the knee-angle hard stop is applied because the restriction improves the transfer of mechanical energy between the shank and thigh. The increased energy transfer allows the hip to reach

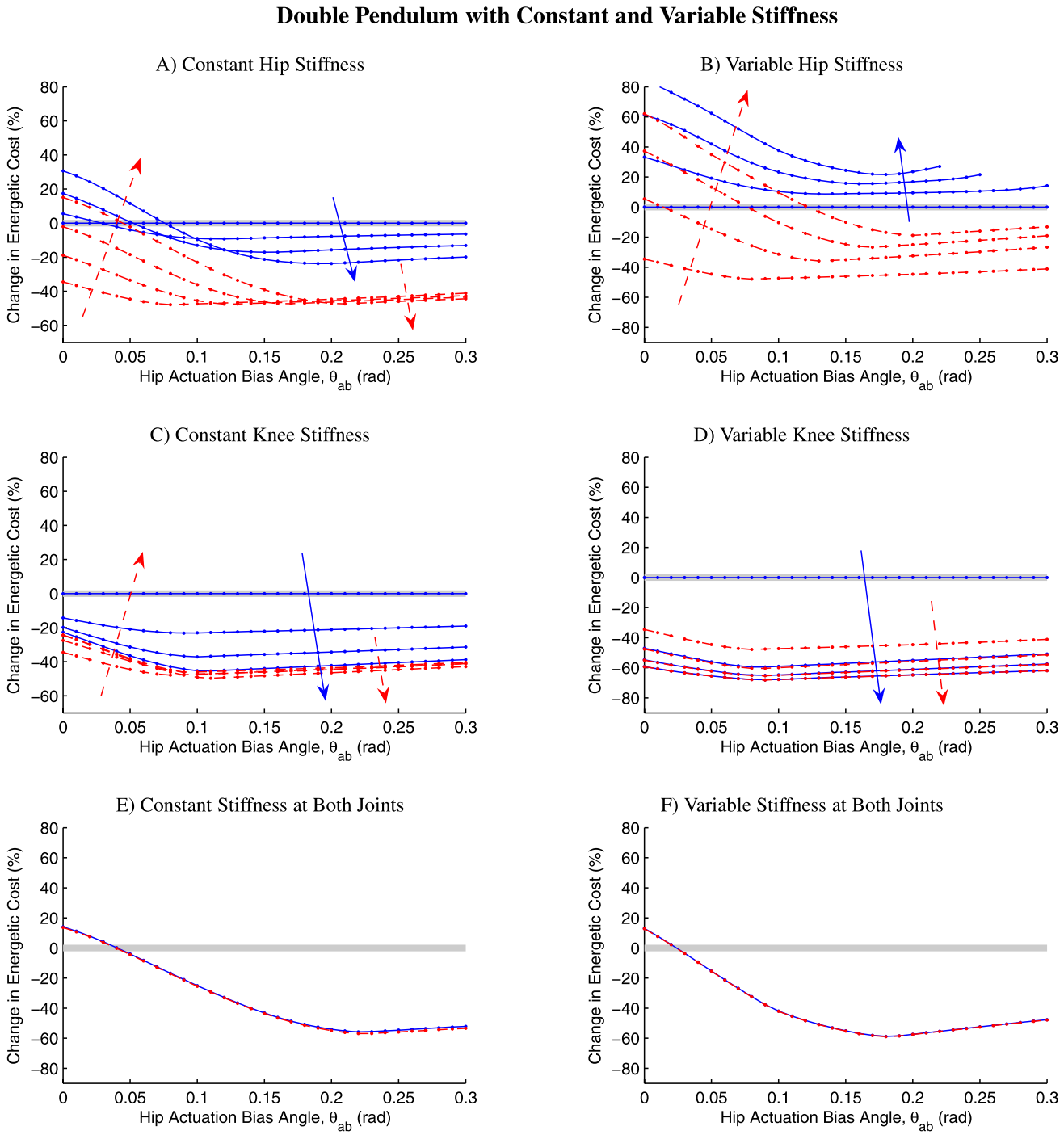

Fig. 7 Effects of constant and variable passive stiffness on the energetic cost of double pendulum swinging. Each trace represents a single set of stiffness parameters and the *arrows* indicate the effect of increasing the stiffness gain from zero to its canonical value (Table 3). *Solid traces* represent the double pendulum experiments performed without the knee-angle hard stop, and dashed traces represent experiments with the hard stop

more flexed angles and centers the hip oscillation closer to θ_{ab}.

The most energetically beneficial operating point for the constant hip stiffness function occurs when the value of $\theta_{\mathrm{sb,h}}$ is large and the value of K_{h} is small. This trend indicates that constant hip torque could produce larger energy reductions than an elastic torque, which changes magnitude as the hip angle varies. A comparison of the relative benefits of using elastic and constant hip torque is shown later in Fig. 8.

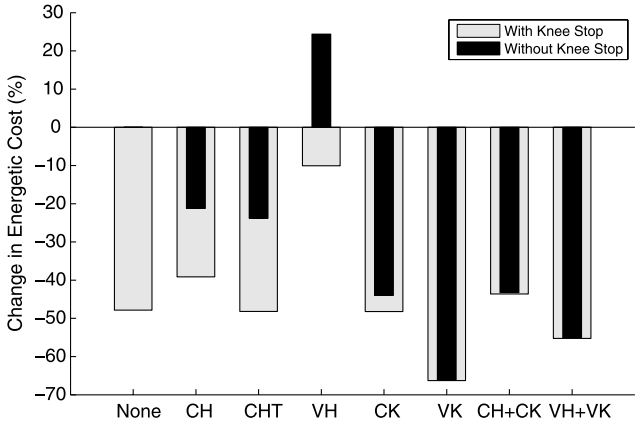

Fig. 8 Comparison of the effects various stiffness implementations have on energetic cost. The energetic cost values were chosen from Fig. 7 at $\theta_{ab} = 0.15$ rad. The labels at the *bottom* of the plot indicate which passive-stiffness implementation was used and are defined as follows: None—no stiffness at either joint, CH—constant hip stiffness, CHT—constant hip torque, VH—variable hip stiffness, CK—constant knee stiffness, VK—variable knee stiffness, CH+CK—constant stiffness at both joints, and VH+VK—variable stiffness at both joints

Variable hip stiffness (Fig. 7B) affects energetic cost in a manner qualitatively similar to that of constant hip stiffness for low values of θ_{ab} (i.e., increasing K_h increases energetic cost). Unlike constant hip stiffness, at higher values of θ_{ab}, variable hip stiffness *increases* energetic cost in a manner directly related to K_h. Although the addition of the knee-angle hard stop reduced the energetic cost, variable hip stiffness consistently produces cost increases that are directly related to stiffness gain. Therefore, at any value of θ_{ab}, the use of variable stiffness at the hip increases energetic cost.

Constant knee stiffness (Fig. 7C) reduces energetic cost for all values of θ_{ab}, and the reduction level is directly related to K_k. The knee-angle hard stop can provide energetic cost benefit, but this effect is limited primarily to low-gain stiffness. Furthermore, once the hard stop has been applied, stiffness does not provide additional benefit of any significance. In these tests, energetic cost reduction is achieved by preventing the knee from hyperextending and therefore promoting the efficient transfer of kinetic energy between the shank and thigh during swinging. The significant benefit of the hard stop arises because this mechanism prevents knee hyperextension by design.

Variable knee stiffness (Fig. 7D) has a similar effect to constant knee stiffness. The level of energetic cost reduction is higher than the constant stiffness case because the variable stiffness trajectory can create high stiffness near the origin without the side effects of either (1) having a large bias angle that hyperflexes the knee or (2) having a large stiffness gain that rigidly holds the knee and prevents natural swing dynamics. As with the constant knee stiffness, the addition of the hard stop does not provide significant benefit.

Figures 7E and 7F show the effect of applying stiffness at both the hip and knee. In both the constant and variable stiffness cases, the application of the knee-angle hard stop had no significant effect. The maximum amount of energetic cost reduction was approximately the same in both cases (57% in the constant stiffness case and 59% in the variable stiffness case). The only difference was that the minima occurred at different values of θ_{ab} (0.18 rad in the constant stiffness case and 0.22 rad in the variable stiffness case).

To quantitatively compare the different methods of applying passive stiffness, we selected the value of the energetic cost in each case at $\theta_{ab} = 0.15$ rad, which is the center of the hip's range of motion during normal human walking (Hurmuzlu et al. 1994). The results (Fig. 8) demonstrate that nearly all of the stiffness implementations are capable of reducing energetic cost. The one exception—variable hip stiffness—does not reduce energetic cost because this implementation produces passive hip torques that decrease significantly as the hip flexes. We found previously that the hip passive-stiffness functions that produce the largest energetic cost reduction have large bias values and small gain values. Because these functions produce torques that remain approximately constant as the hip rotates, we sought to maximize the energetic cost reduction by replacing the passive stiffness with a constant torque. The results show that without the knee-angle hard stop, variable stiffness, which has a small bias angle of 0.70 rad, increases energetic cost by 24%; constant hip stiffness, which has a large bias angle of 12.00 rad, reduces energetic cost by 21%; and a constant hip torque of 3.80 Nm, which can be considered a stiffness function with infinitely large bias angle, reduces energetic cost by 24%.

The largest energetic cost reduction in these experiments was achieved using variable knee stiffness. Because these results depend on the choice of canonical parameters, the more important observations are that (1) mechanisms that restrict the knee from hyperextending—the knee-angle hard stop, constant knee stiffness, and variable knee stiffness—can provide significant reduction in energetic cost and (2) hip elasticity with a low bias angle can increase energetic cost.

5.3 Robotic leg validation

All analysis in this study was performed using our computational model of leg swinging because this approach provides a fast and relatively simple means of exploring the role of a wide-range of parameters. Additionally, computational models offer the unique ability to measure performance quantities non-invasively and without expensive hardware. Experimentation with the physical robotic model is crucial, however, to physically validate the experimental results in an environment subject to noise, difficult-to-model friction, and real-world limitations on the system's actuators and sensors. Because robotic experiments take significantly more

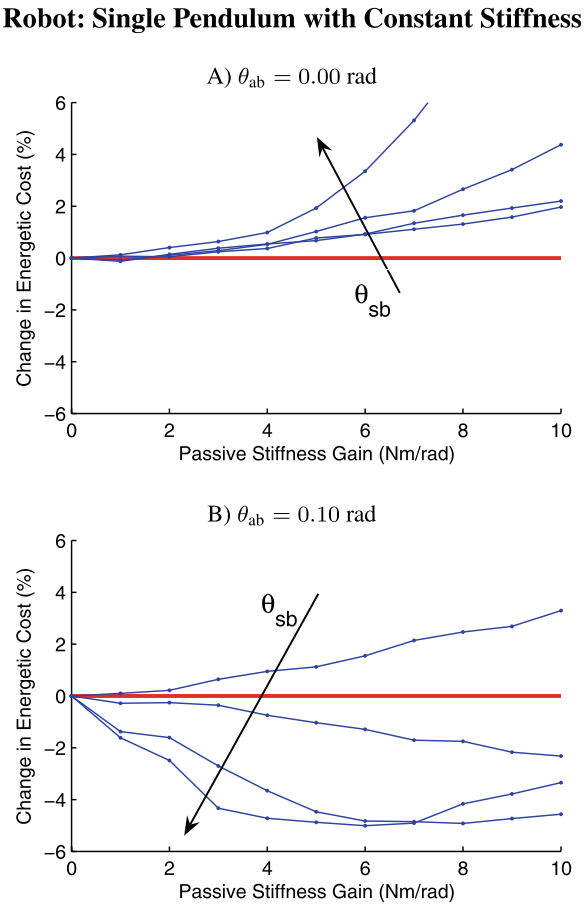

Fig. 9 Robotic validation of data presented in Fig. 3 demonstrating that passive joint stiffness only produces energetic cost reduction in the single pendulum system when actuation bias angle is non-zero. The individual traces in each plot correspond to fixed values of θ_{sb}. The *arrows* indicate the effect of increasing θ_{sb} from 0.00 to 0.45 rad in increments of 0.15 rad. The computational model used the following parameter values: $\theta_{ab} = 0.00$, 0.15 rad; $K = 0.0$–50.0 Nm/rad; and $\theta_{sb} = 0.0$–1.0 rad

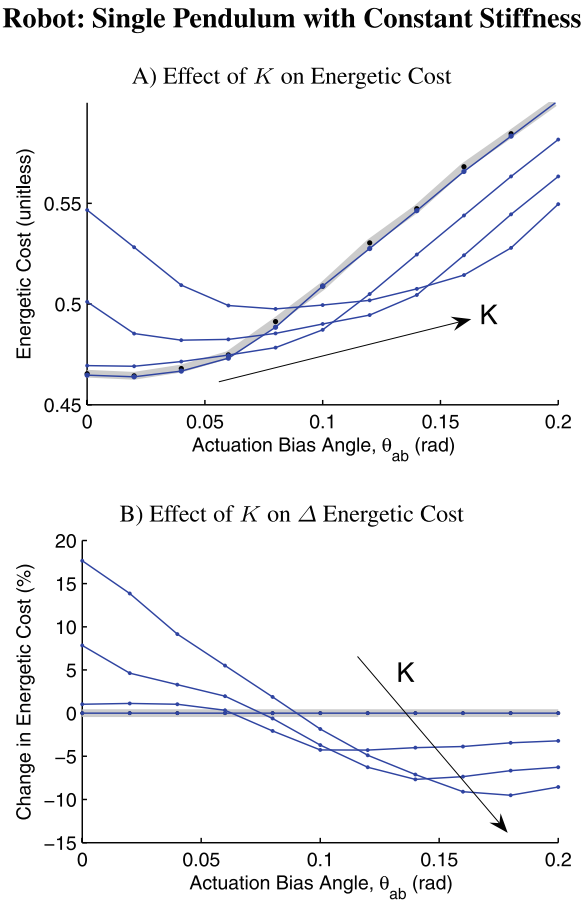

Fig. 10 Robotic validation of data presented in Fig. 4 demonstrating that the total energetic cost reduction in the single pendulum system is a function of θ_{ab} and θ_{sb}. In each plot, the traces correspond to fixed values of K, and the *arrows* indicate the effect of increasing K from 0.0 to 12.0 Nm/rad in increments of 4.0 Nm/rad. The computational model used the following parameter values: $\theta_{ab} = 0.00$–0.30 rad; $K = 0.0$–21.0 Nm/rad; and $\theta_{sb} = 0.45$ rad

time to run than computational experiments (the computational model runs at ∼25× real time), we did not replicate all experimental data. Rather, we chose to validate sample experiments for both the single- and double-pendulum systems. Figure 9 replicates the results of Fig. 3, which demonstrates that a non-zero actuation bias angle, θ_{ab}, is required for passive joint stiffness to produce energetic cost reductions in a single pendulum. Figure 10 replicates the results of Fig. 4, which demonstrates that the amount of energetic cost reduction in a single pendulum is a function of the passive-stiffness gain and the actuation bias angle. (It is also a function of the passive-stiffness bias angle but these results were not replicated.) Finally, Fig. 11 replicates the results from Fig. 6, which presents the effects of varying the hip and knee passive-stiffness bias angles on the energetic cost reduction in the double pendulum.

The qualitative trends in each robotic data figure correspond well their computational counterparts. The primary difference in the data was that the energetic cost reduction was smaller in the robotic experiments than in the computational experiments. This difference resulted from a limit we encountered in the total amount of torque the joint actuators could produce. In a production-level robot, the passive torques would be applied by passive elastic components, but our choice to use *virtual model control* in this lab-based system required that the actuators produce both the active and passive torques. As a result, we reduced the total torque demand on the actuators by limiting the range of parameters tested. Nonetheless, despite the physical limitations of our robotic implementation, the data presented in this section validates that passive joint stiffness can reduce energetic cost in robotic leg swinging.

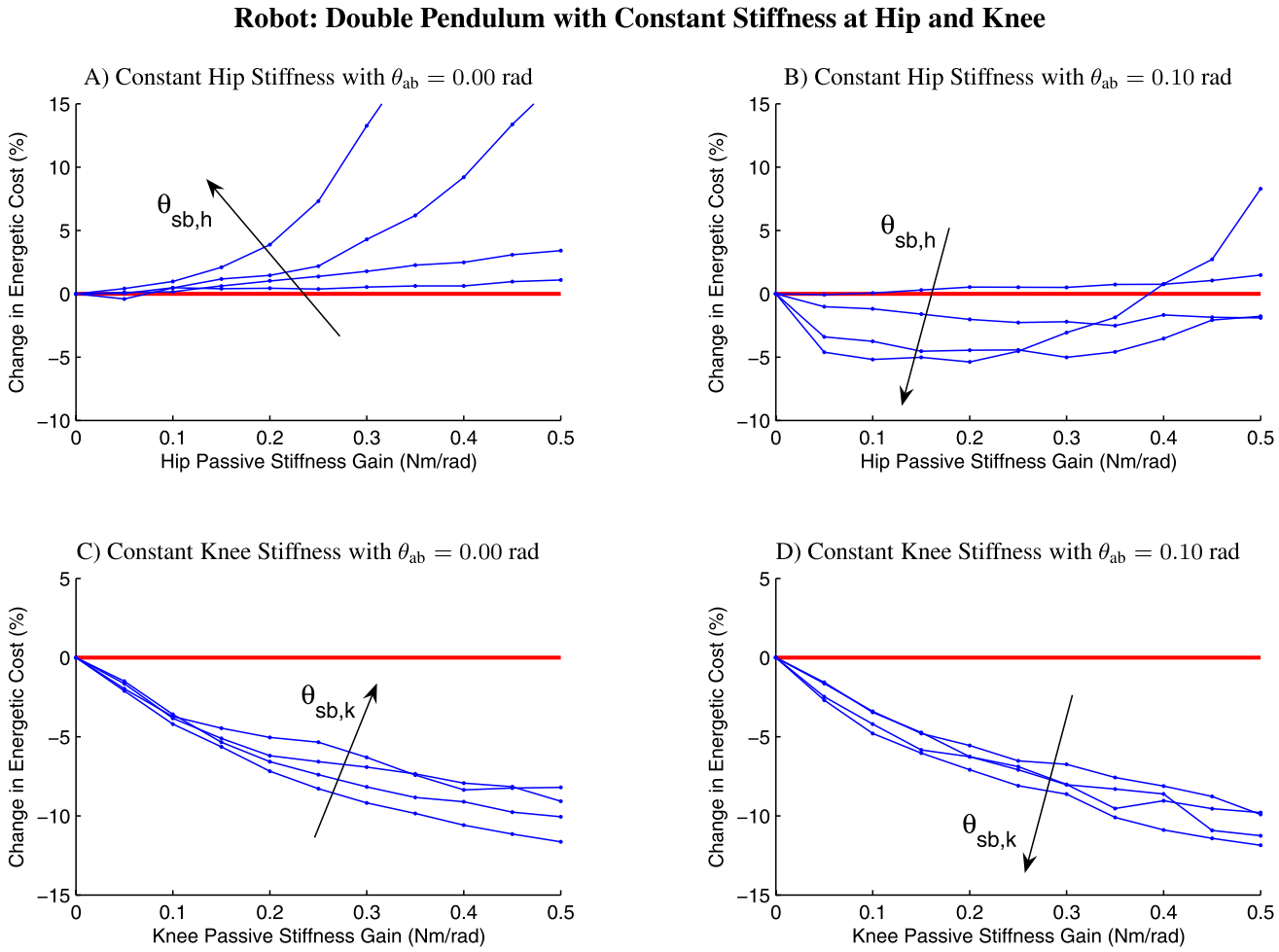

Fig. 11 Robotic validation of data presented in Fig. 6. Passive hip stiffness only improves the energetic cost of double pendulum swinging when the actuation bias angle is non-zero (**A** and **B**). Passive knee stiffness can reduce energetic cost regardless of actuation bias angle; nonzero values of $\theta_{sb,k}$ produce less energetic cost reduction when θ_{ab} is zero and produce more when θ_{ab} is non-zero (**C** and **D**). In Plots (**A**) and (**B**), the traces correspond to fixed values of $\theta_{sb,h}$, and the *arrows* indicate the effect of increasing $\theta_{sb,h}$ from 0.0 to 12.0 rad in increments of 4.0 rad. The corresponding parameters used in the computational model were: $\theta_{ab} = 0.00$, 0.15 rad; $K = 0.0$–1.0 Nm/rad; and $\theta_{sb} = 0.0$–12.0 rad. In Plots (**C**) and (**D**), the traces correspond to fixed values of $\theta_{sb,k}$, and the *arrows* indicate the effect of increasing $\theta_{sb,k}$ from 0.0 to 0.6 rad in increments of 0.2 rad. In this case, the corresponding parameters used in the computational model were: $\theta_{ab} = 0.00$, 0.15 rad; $K = 0.0$–5.0 Nm/rad; and $\theta_{sb} = 0.0$–0.6 rad

6 Discussion

In this paper, we demonstrated that emulating the physiological use of passive stiffness in passive-dynamic robots can reduce the energetic cost of leg swinging without significantly affecting stability. Using a single-joint pendulum, we showed that both constant and variable passive-stiffness functions are capable of reducing the energetic cost but that the variable stiffness provides no benefit that warrants its complicated implementation. Using the double pendulum, we showed that knee stiffness, especially that which prevents knee hyperextension, provides the largest energetic cost reduction.

We tested the system with two types of passive elastic elements—constant stiffness springs and a physiologically based variable stiffness trajectory. In the development of walking robots, the use of constant stiffness is preferable because it can be implemented easily by attaching linear elastic elements (e.g., off-the-shelf springs) about a joint such that they apply torque in parallel with the actuators. The disadvantage to using constant elasticity is that the designer is forced to choose one stiffness value that is acceptable for all leg configurations and at all phases of movement. Alternatively, variable stiffness components produce joint torque as a function of joint angle in a physiological manner, but their implementation in robotic systems is significantly more complicated. We avoided the implementation obstacle

in this research by using *virtual model control* to actively implement all forms of passive stiffness. (We did not consider the energy used to virtually implement the passive-stiffness components when calculating energetic cost.)

We hypothesized that passive stiffness at the hip could reduce energetic cost by countering the gravitational torque and, therefore, reducing the actuator load. Using both the single and double pendulum models, we determined that this hypothesis is valid only when the hip actuation bias angle does not correspond to the direction of gravity ($\theta_{ab} \neq 0$ rad). Furthermore, using the double pendulum, we found that the hip stiffness function that produced the lowest energetic cost had a high stiffness bias angle and a low stiffness gain value. This type of function most closely resembles a constant torque because the joint angle does not significantly affect torque level. In comparing constant stiffness, variable stiffness, and constant torque, we found that the level of energetic cost savings was highly dependent on bias angle. Variable stiffness, which has a relatively low bias angle, increased energetic cost; constant stiffness, which has a high bias angle, decreased energetic cost significantly; and constant torque provided the maximum cost decrease.

We also hypothesized that passive stiffness at the knee could reduce energetic cost by promoting the transfer of kinetic energy between the shank and thigh during swinging. We found that energy transfer improved with all mechanisms that restrict knee hyperextension, including the constant stiffness, the variable stiffness, and the knee-angle hard stop. In our experiments, variable knee stiffness provided the largest reduction in energetic cost. A post-hoc analysis showed that the reason for the superior performance of the variable stiffness function was that it is essentially a combination of a constant knee stiffness (biased about $\theta_k = 0.29$ rad) and an exponential-stiffness knee stop. The constant stiffness component increases the magnitude of knee flexion during swing, which increases the shank's kinetic energy at knee extension; the hard stop component improves the amount of this kinetic energy that is transferred to the thigh. Increasing the level of thigh kinetic energy reduces energetic cost because larger-amplitude leg swinging is produced.

Passive-stiffness properties were found to also benefit the energetic cost of leg swinging by preventing non-conservative collisions at knee strike. The elastic hard stop used in these experiments passively stores potential energy as the knee reaches its extension limit during forward (anterior) swinging. This energy is then released during backward (posterior) swinging to produce increased knee flexion. Passive-dynamic walking robots commonly allow the shank to swing forward until it impacts a rigid limit created by the physical construction of the knee. At impact, kinetic energy is dissipated, and a latch engages that prevents the knee from flexing during stance (Collins and Ruina 2005; Wisse et al. 2007). By reusing rather than dissipating energy, out method reduces the energetic cost of leg swinging by approximately 7%.[3]

We found that variable stiffness at either joint during leg swinging does not present a benefit that justifies its more complex implementation because (1) the variable hip stiffness actually increases energetic cost and (2) the performance of the variable knee stiffness can be theoretically reproduced by altering the parameters of the linear stiffness and exponential hard stop functions (data not shown). In a true mechanical implementation, however, nonlinear elastic components may still be necessary to implement the exponential knee-stop stiffness.

Using the variable stiffness functions as models of human joint stiffness, our experimental data suggest that the energetic cost of human leg swinging is decreased by passive knee stiffness and increased by passive hip stiffness. A likely explanation for the poor performance of the hip stiffness in our experiments is that the human leg's passive-stiffness properties are better tuned to the swing phase of walking rather than to the more uncommon behavior of isolated leg swinging. The primary difference between these behaviors is that, in the swing phase of walking, the leg acquires much of its needed energy from ankle plantarflexion; in isolated swinging, the leg relies solely on less-efficient hip flexion. Because the leg receives a large burst of mechanical energy from plantarflexion, passive hip stiffness torque attenuates as the hip flexes, and a small burst of hip extension torque is used to actively stiffen the joint and prevent hyperflexion (Doke et al. 2005). The swinging leg model does not include plantarflexion. As a result, passive hip stiffness maintains large-amplitude oscillations by continuing to produce flexion torque during late swing rather than attenuating. This behavior corresponds to high-bias stiffness or a continuous torque.

Although this study focused on the task of leg swinging, our results suggest that passive-stiffness properties would also increase the energy efficiency of walking. Previous studies have shown that the metabolic cost of leg swinging during walking is 10% (Gottschall and Kram 2005) and the metabolic cost of propulsion is 48% (Grabowski et al. 2005). This research has shown that the energetic cost of leg swinging can be reduced 66% by using passive stiffness at the knee alone. Furthermore, passive knee stiffness could also reduce the energetic cost of propulsion in walking because the energy stored during late swing (i.e., knee extension) could contribute directly to propulsion during mid- to late-stance. A significant limitation in relating our experimental approach to walking is that we did not include the

[3]This comparison was made using a simulation of the double pendulum model in which the elastic hard stop was replaced with the impact model from Marhefka and Orin (1999) using $n = 1$, $k = 50000$ Nm/rad, and $\alpha = 0.4$.

ankle, which provides the largest amount of passive energy storage during walking. We chose to ignore the ankle because its role is insignificant in no-contact swinging. However, the Achilles tendon has been shown to passively store and reuse up to 50% of the body's mechanical energy during walking (Sasaki and Neptune 2006). Therefore, in addition to lowering the energetic cost of leg swinging by 66%, we expect that passive elasticity can significantly reduce the energetic cost of propulsion in walking.

In summary, we have demonstrated that passive joint stiffness can be used to reduce the energetic cost of robotic leg swinging. We have validated our hypotheses (1) that hip stiffness can reduce energetic cost by producing anti-gravity torques that lower the amount of required actuator work (provided a high stiffness bias angle was used) and (2) that knee stiffness can reduce energetic cost by promoting the efficient transfer of kinetic energy between the shank and thigh at knee extension. Experiments were performed using a computational model and were validated using a full-scale robotic leg. Physiological models of human joint stiffness proved beneficial at the knee and detrimental at the hip. Constant stiffness combined with a limit on knee hyperextension produced comparable results to the physiological stiffness model without requiring complicated implementation techniques. We expect that passive energy storage will be more effective in walking because the amount of passive energy stored in the ankle is significantly larger than that stored in the hip and knee.

Acknowledgements This research was supported by National Science Foundation (NSF) grant #0131612, by an NSF Graduate Research Fellowship to S. Migliore, by the Center for Behavioral Neuroscience (an NSF Science and Technology Center), and by the Georgia Research Alliance. Corporate donations were received from AMC, Inc. and dSpace, Inc.

References

Abe, M. O., & Yamada, N. (2003). Modulation of elbow stiffness in a vertical plane during cyclic movement at lower or higher frequencies than natural frequency. *Experimental Brain Research*, *153*(3), 394–399.

Alexander, R. M., & Bennet-Clark, H. C. (1977). Storage of elastic strain energy in muscle and other tissue. *Nature*, *265*, 114–117.

Blickhan, R. (1989). The spring-mass model for running and hopping. *Journal of Biomechanics*, *22*(11–12), 1217–1227.

Brinckmann, P., Frobin, W., & Leivseth, G. (2002). *Musculoskeletal biomechanics*. New York: Thieme.

Brown, T. G. (1914). On the nature of the fundamental activity of the nervous centres; together with an analysis of rhythmic activity in progression, and a theory of the evolution of function in the nervous system. *Journal of Physiology*, *48*, 18–46.

Cavagna, G. A., & Margaria, R. (1966). Mechanics of walking. *Journal of Applied Physiology*, *21*, 271–278.

Collins, S. H., & Ruina, A. (2005). A bipedal walking robot with efficient and human-like gait. In *Proceedings of the 2005 IEEE international conference on robotics and automation* (pp. 1995–2000). Barcelona, Spain, April 2005.

Doke, J., Donelan, J. M., & Kuo, A. D. (2005). Mechanics and energetics of swinging the human leg. *Journal of Experimental Biology*, *208*, 439–445.

Endo, G., Nakanishi, J., Morimoto, J., & Cheng, G. (2005). Experimental studies of a neural oscillator for biped locomotion with QRIO. In *Proceedings of the 2005 IEEE international conference on robotics and automation* (pp. 598–604). Barcelona, Spain, April 2005.

English, C. E., & Russell, D. (1999). Implementation of variable joint stiffness through antagonistic actuation using rolamite springs. *Mechanism and Machine Theory*, *34*, 27–40.

Gottschall, J. S., & Kram, R. (2005). Energy cost and muscular activity required for leg swing during walking. *Journal of Applied Physiology*, *99*, 23–30.

Grabowski, A., Roberts, T. J., & Kram, R. (2005). Metabolic cost of generating muscular force in human walking: Insights from load-carrying and speed experiments. *Journal of Applied Physiology*, *98*, 579–583.

Hatsopoulos, N. G. (1996). Coupling the neural and physical dynamics in rhythmic movements. *Neural Computation*, *8*, 567–581.

Hill, A. V. (1970). *First and last experiments in muscle mechanics*. Cambridge: Cambridge University Press.

Hirai, K., Hirose, M., Haikawa, Y., & Takenaka, T. (1998). The development of the Honda humanoid robot. In *Proceedings of the 1998 IEEE international conference on robotics and automation* (pp. 1321–1326). Leuven, Belgium, May 1998.

Hof, A. L. (1990). *Multiple muscle systems: biomechanics and movement organization*. New York: Springer.

Hurmuzlu, Y., Basdogan, C., & Carollo, J. C. (1994). Presenting joint kinematics of human locomotion using phase plane portraits and Poincaré maps. *Journal of Biomechanics*, *27*(12), 1495–1499.

Kaneko, K., Kanehiro, F., Kajita, S., Hirukawa, H., Kawasaki, T., Hirata, M., Akachi, K., & Isozumi, T. (2004). Humanoid robot HRP-2. In *Proceedings of the 2004 IEEE international conference on robotics and automation* (pp. 1083–1090). New Orleans, LA, April 2004.

Ker, R. F., Bennett, M. B., Bibby, S. R., Kester, R. C., & Alexander, R. M. (1987). The spring in the arch of the human foot. *Nature*, *325*, 147–149.

Kim, J.-Y., Park, I.-W., Lee, J., Kim, M.-S., Cho, B.-K., & Oh, J.-H. (2005). System design and dynamic walking of humanoid robot KHR-2. In *Proceedings of the 2005 IEEE international conference on robotics and automation* (pp. 1443–1448). Barcelona, Spain, April 2005.

Kolacinski, R. M., & Quinn, R. D. (1998). A novel biomimetic actuator system. *Robotics and Autonomous Systems*, *25*, 1–18.

Kram, R., & Taylor, C. R. (1990). Energetics of running: a new perspective. *Nature*, *346*, 220–221.

Loffler, K., Gienger, M., & Pfeiffer, F. (2002). Model based control of a biped robot. In *Proceedings of the 7th international workshop on advanced motion control* (pp. 443–448). May 2002.

Marhefka, D. W., & Orin, D. E. (1999). A compliant contact model with nonlinear damping for simulation of robotic systems. *IEEE Transactions on Systems, Man, and Cybernetics. Part A, Systems and Humans*, *29*(6), 566–572.

Matsuoka, K. (1985). Sustained oscillations generated by mutually inhibiting neurons with adaptation. *Biological Cybernetics*, *52*, 367–376.

Matsuoka, K. (1987). Mechanisms of frequency and pattern control in the neural rhythm generators. *Biological Cybernetics*, *56*, 345–353.

McGeer, T. (1990a). Passive dynamic walking. *International Journal of Robotics Research*, *9*(2), 62–82.

McGeer, T. (1990b). Passive dynamic walking with knees. In *Proceedings of the 1990 IEEE international conference on robotics and automation* (pp. 1640–1645). Cincinnati, OH, April 1990b.

McMahon, T. A., Valiant, G., & Frederick, E. C. (1987). Groucho running. *Journal of Applied Physiology*, *62*(6), 2326–2337.

Migliore, S. A. (2008). *The role of passive joint stiffness and active knee control in robotic leg swinging: applications to dynamic walking*. PhD thesis, Georgia Inst. of Tech., Atlanta, GA, April 2008.

Migliore, S. A., Brown, E. A., & DeWeerth, S. P. (2005). Biologically inspired joint stiffness control. In *Proceedings of the 2005 IEEE international conference on robotics and automation* (pp. 4519–4524). Barcelona, Spain, April 2005.

Migliore, S. A., Brown, E. A., & DeWeerth, S. P. (2007). Novel nonlinear elastic actuators for passively controlling robotic joint compliance. *ASME Journal of Mechanical Design*, *129*(4), 406–412.

Nayfey, A. H., & Balachandran, B. (1995). *Applied nonlinear dynamics*. New York: Wiley-Interscience.

Ogura, Y., Aikawa, H., Lim, H., & Takanishi, A. (2004). Development of a human-like walking robot having two 7-DoF legs and a 2-DoF waist. In *Proceedings of the 2004 IEEE international conference on robotics and automation* (pp. 134–139). New Orleans, LA, April 2004.

Piazza, S. J., & Delp, S. L. (1995). The influence of muscles on knee flexion during the swing phase of gait. *Journal of Biomechanics*, *29*(6), 723–733.

Pratt, G. A., & Williamson, M. M. (1995). Series elastic actuators. In *Proceedings of the 1995 IEEE/RSJ international conference on intelligent robots and systems* (Vol. 1, pp. 399–406). Pittsburg, PA, July 1995.

Pratt, J., Dilworth, P., & Pratt, G. (1997). Virtual model control of a bipedal walking robot. In *Proceedings of the 1997 IEEE international conference on robotics and automation* (pp. 193–198). Albuquerque, NM, 1997.

Riener, R., & Edrich, T. (1999). Identification of passive elastic joint moments in the lower extremities. *Journal of Biomechanics*, *32*, 539–544.

Robinson, D. W., Pratt, J. E., Paluska, D. J., & Pratt, G. A. (1999). Series elastic actuator development for a biomimetic walking robot. In *Proceedings of the 1999 IEEE/ASME international conference on advanced intelligent mechatronics* (pp. 561–568). September 1999.

Rossignol, S. (1996). *Handbook of physiology. Neural control of stereotypic limb movements* (pp. 173–216). New York: The American Physiological Society. Chap. 5.

Sasaki, K., & Neptune, R. R. (2006). Muscle mechanical work and elastic energy utilization during walking and running near the preferred gait transition speed. *Gait and Posture*, *23*, 383–390.

Simoni, M. (2002). *Synthesis and analysis of a physical model of biological rhythmic motor control with sensorimotor feedback*. PhD thesis, Georgia Inst. of Tech., April 2002.

Sparrow, W. A., Hughes, K. M., Russell, A. P., & Rossignol, P. F. (2000). *Energetics of human activity*. Human Kinetics, Chicago, 2000.

Strogatz, S. H. (1994). *Nonlinear dynamics and chaos*. Cambridge: Perseus Books. ISBN 0-7382-0453-6.

Wheeless, C. (2005). *Wheeless' textbook of orthopaedics*. Data Trace Publishing Company, http://www.wheelessonline.com. Book online. Retrieved October 3, 2006.

Williams, C. A., & DeWeerth, S. P. (2007). A comparison of resonance tuning with positive versus negative sensory feedback. *Biological Cybernetics*, *96*(6).

Williamson, M. M. (1995). *Series elastic actuators*. Master's thesis, Mass. Inst. Technol., January 1995.

Williamson, M. M. (1999). *Robot arm control exploiting natural dynamics*. PhD thesis, Mass. Inst. Technol.

Wisse, M., Guillaume, F., Frankenhuyzen, J. V., & Moyer, B. (2007). Passive-based walking robot. *IEEE Robotics and Automation Magazine*, *14*(2), 52–62.

Yamaguchi, J., & Takanishi, A. (1997). Design of biped walking robots having antagonistic driven joints using nonlinear spring mechanism. In *Proceedings of the 1997 IEEE/RSJ international conference on intelligent robots and systems* (Vol. 1, pp. 251–259). Grenoble, France, September 1997.

Shane A. Migliore's research interests include the design and control of both robotic systems and aerospace vehicles with an emphasis on actuation systems. He received the B.S. degree in biomedical engineering from Boston University in 2001 and the M.S. and Ph.D. degrees in electrical and computer engineering from the Georgia Institute of Technology in 2004 and 2008, respectively.

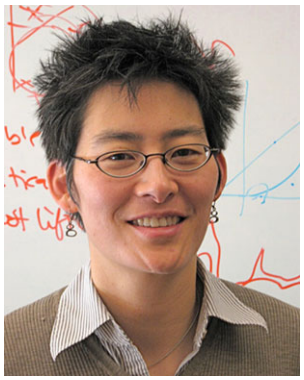

Lena H. Ting is an Associate Professor in the Wallace H. Coulter Department of Biomedical Engineering at the Georgia Institute of Technology and Emory University. She studies the neuromechanical control of balance and locomotion in humans and animals. She received the B.S. degree in mechanical engineering from the University of California, Berkeley, in 1990, the M.S.E. degree in biomechanical engineering from Stanford University in 1993 and the Ph.D. degree in mechanical engineering from Stanford University in 1998.

Stephen P. DeWeerth is a Professor in the Wallace H. Coulter Department of Biomedical Engineering and in the School of Electrical and Computer Engineering at the Georgia Institute of Technology and the Emory University. His research emphasizes the development of systems that are inspired by and interfaced to neurobiology. His research group develops real-time computational and robotic systems that model biological motor control including rhythmic motor-pattern generation and sensorimotor feedback, and implements electronics and signal-processing circuitry to interface these systems to neural tissue and to muscles. He received the M.S. degree in computer science and the Ph.D. degree in computation and neural systems from the California Institute of Technology, Pasadena, in 1987 and 1991, respectively.